Chapter 6
Energy Changes in Photosynthetic Electron Transport: Probing Photosynthesis by Pulsed Photoacoustics

David Mauzerall and Steven P. Mielke

Abstract Pulsed photoacoustics (PPA) is the ideal method for determining the thermodynamics and energy-storage (E-S) efficiency of photosynthesis. In particular it is applicable to whole cells, and so allows direct study of in vivo energy storage by PSI and PSII, avoiding artifacts resulting from damage to isolated photosystems and disruption of linear electron flow. It is the in vivo efficiency that ultimately limits energy storage at limiting light intensities. In this chapter, after discussing advantages of separating the enthalpic and entropic contributions to free energy changes of photochemistry, we describe PPA methodology in detail, and discuss information available from the enthalpies it provides. To illustrate the use of PPA to obtain E-S efficiencies in vivo, we then describe a comprehensive study of cyanobacterial whole cells in the far-red spectral region. This study has resulted in the clear differentiation of the contributions of PSI and PSII to the observed efficiency; the first identification of the trap energies of both systems directly from enthalpy measurements; and quantification of the thermodynamically required decay in storage for excitations below these energies. This unique and elegant biophysical method can additionally provide such key information as volume changes resulting from electron transfer, optical cross sections, quantum yields, and turnover times.

Keywords Thermodynamics • Electron transfer • Photoacoustics • Enthalpy • Energy-storage efficiency • Oxygenic photosynthesis • *Acaryochloris marina* • Chlorophyll *d*

D. Mauzerall (✉) • S.P. Mielke
Laboratory of Photobiology, The Rockefeller University,
1230 York Avenue, 10065 New York, NY, USA
e-mail: mauzera@mail.rockefeller.edu

J. Golbeck and A. van der Est (eds.), *The Biophysics of Photosynthesis*,
Biophysics for the Life Sciences 11, DOI 10.1007/978-1-4939-1148-6_6,

Abbreviations

Am	*Acaryochloris marina*
Chl	Chlorophyll
E-S	Energy-storage
PA	Photoacoustics
PPA	Pulsed photoacoustics
PSI	Photosystem I
PSII	Photosystem II
Sl	*Synechococcus leopoliensis*

6.1 Introduction

Full understanding of a process requires knowledge of both its thermodynamics and its kinetics. Extensive spectroscopic investigations have led to good knowledge of the intermediates and kinetics of photosystem I (PSI) and photosystem II (PSII) (see Chaps. 8 and 10 of this volume). Further, the successful determination of the structure of reaction centers and antenna proteins (see Chaps. 1 and 11 of this volume) has added much to our understanding of electron transport in both photosystems. However, knowledge of the thermodynamics of this process is far less advanced.

Since the early photosynthetic reactions are electron-transfer processes, focus has been placed on the redox potentials of the intermediates. As discussed below, values of these potentials are not known at all well. There are two principal reasons for wishing to know redox potentials of the electron-transport cofactors more accurately. One is the far greater understanding obtained by separating the free energy change into its bonding (enthalpic) and structural (entropic) components. Aside from the concentration term, the latter is small in many chemical reactions at normal temperature, ~300 K. However, in structured environments such as proteins in the particular solvent, water, the contribution of entropy can be the determining factor. (This is exemplified by protein denaturation, where the massive configuration entropy determines the irreversible thermal reaction.) From the viewpoint of statistical mechanics, a further breakdown of the free energy into the change in heat capacity at each reaction step is the most useful. Unfortunately, we are still quite a ways from the precise measurements required for such detailed knowledge of the intermediates. Nevertheless, knowledge of the enthalpy and entropy from accurate thermodynamic measurements provides important insights into the processes involved in electron transfer.

The second reason to accurately know the thermodynamics of electron transfer is that it provides information on the efficiency. In the context of photosynthesis, the word "efficiency" is used with several different meanings [1, 2]. It often refers to the "solar-energy conversion efficiency," or that fraction of incident solar energy that is absorbed by the system and ultimately stored in chemical form [1, 3]. This is

a small and variable number. It is variable because incident photon flux densities are affected by the diurnal cycle, changes in cloud cover, physical differences among local environments, etc. It is small because about half the solar spectrum is in the infrared region, and therefore not used in photosynthesis. Moreover, for absorbed shorter wavelength photons that are used, all energy exceeding that of the reaction center traps is rapidly degraded to heat. (This fast degradation of surplus energy is a characteristic of all photon-driven systems, including photocells. Photothermal devices maximize this effect by converting all the photon energy to heat.) Thus, only a small fraction of incident solar energy is captured and converted by the reaction centers—perhaps 1 or 2 % in higher plants under typical conditions [4].

This chapter focuses on the "energy-storage efficiency," ε_{ES}, or that fraction of the *absorbed* energy that is converted and stored. This quantity is a function of time, reaching a minimum when the final products of photosynthesis are reached. Our primary subject is the determination of ε_{ES} from enthalpies obtained using pulsed photoacoustics (PPA). PPA is unique among biophysical methods of photosynthesis research in that, rather than providing spectroscopic or kinetic information from which the details of photochemistry must be inferred, it measures changes in *energy* (enthalpy) resulting from electron-transfer reactions, directly providing detailed thermodynamic and other basic information that is difficult to obtain by other means. Examples include changes in volume and entropy [5–7], turnover times and quantum yields [7, 8], optical cross sections and energy-storage efficiencies [8], and, from the latter, trap energies and spectral dependence of uphill energy transfer [9].

In Sect. 6.2, we discuss what is currently known of the free energies of electron transport. Biophysical methods of measuring the enthalpy are discussed in Sect. 6.2.1, and what can be learned from knowledge of enthalpy and entropy changes is discussed in Sect. 6.2.2. In Sect. 6.3, we concentrate on PPA—one of only a few available methods for directly obtaining the enthalpy—emphasizing accurate in vivo measurements that allow determination of the millisecond time scale ε_{ES} and other key photosynthetic quantities. PPA methodology and what can be learned by this method are discussed in Sect. 6.3.1. An example of determining several useful parameters of photosynthesis in the Chl *d*-utilizing organism *Acaryochloris marina*, as well as in the Chl *a* species *Synechococcus leopoliensis*, is given in Sect. 6.3.2. Finally, in Sect. 6.4, we offer some concluding remarks.

6.2 Decomposition of Free Energy into Enthalpy and Entropy

The redox potentials (free energies, ΔG) of the steps in the PSI and PSII electron-transfer pathways are in general not very accurately known, because of the limitations of methodology and variability of the preparations. We previously

concluded that for PSI the potentials are known only to within ±0.05 V (eV) [10]. The uncertainties arise primarily because of mismatch of time scales—minutes for measurements (typically standard-state redox titrations) and less than microseconds for the actual reactions. This mismatch opens the possibility that equilibrium measurements do not accurately capture non-equilibrium in vivo processes. In addition, the measurements allow only one of the pair of products to be measured. The range of values observed for the intermediates allows a compromise between maximizing the energy-use efficiency and preserving adequate forward electron flow to products. In vivo measurements of ΔG are preferable to in vitro measurements, but, when possible, require more difficult methods.

The Gibbs free energy is given by the well-known expression

$$\Delta G = \Delta H - T\Delta S, \tag{6.1}$$

where T is the absolute temperature and ΔG, ΔH, and ΔS are changes in free energy, enthalpy, and entropy for reactions in a closed system at constant pressure. Given Eq. (6.1) (and that entropy meters are hard to come by!), a simple method for determining the change in entropy is to measure ΔH, and then calculate ΔS by difference with ΔG. The justification for treating the measured values as standard-state values is given in [11]. Before discussing specific methods for obtaining ΔH, we make the following comments:

1. The photosynthetic system is obviously "open"; that is, energy flows into and out of the system throughout the sequence of reaction steps. Yet we are treating it as a closed system at equilibrium. This is a fair approximation for light intensities well below saturation or for single-turnover flashes, where only one electron per unit is being transferred. The electron flow will lead to a potential drop across the organized system, the components of which span a biological membrane in their in vivo state. For liposomal or in vivo systems, the resulting transmembrane potential must be included in the estimated potential. More importantly, there is the question of whether the "completely relaxed" (equilibrium) state of the protein is achieved between each electron-transfer step. If equilibrium is reached, then all is well. If not, then a new state must be defined. Since the thermalization time of small molecules in condensed phases is very fast, any step that lasts beyond a few picoseconds can be defined as a "thermal equilibrium" state; however, if it is not the completely relaxed state, as in reactions with proteins, then it must be carefully distinguished from the true equilibrium state [12–16]. At the moment this issue is not resolved.
2. It is important to remember that it is changes of the thermodynamic parameters that are relevant, and that these changes are a function of temperature, pH, ionic strengths, and, unfortunately, the preparation from which they are obtained. This is another reason why in vivo measurements are particularly useful (Sect. 6.3.1).
3. All the thermodynamic parameters in Eq. (6.1) can be related to changes in heat capacity, ΔC_P. Unfortunately, the time resolution of current heat capacity measurements is insufficient for the transient intermediates under discussion; thus, obtaining the corresponding parameters from their relationship to ΔC_P is not yet feasible.

6.2.1 Methods of Measuring Enthalpy

Indirect method. The temperature dependence of the yield of delayed light from previously excited reaction centers of *R. sphaeroides* has been used by Arata and Parson [17] to estimate the enthalpy of the charge-separation reaction. The basic assumption is that the ion pair is in equilibrium with the singlet excited state. However, there are many other states involved, such as triplets, and the detailed kinetics are always observed to be rather complex. This approach has been criticized on these grounds by Brettel [18] and by McMahon et al. [19].

Direct methods: Photoacoustics. The only available methods for directly measuring the heat evolved (ΔH) in photochemical processes are photoacoustics (PA) and the related thermal deflection [20] and transient grating [21] methods. Here we concentrate on PA, since it is the method with which we have experience, and with which most of the information on photosynthetic systems has been obtained. PA methodology is well described in the literature [22–28]; therefore, in the following section we focus on *pulsed* photoacoustics (PPA), emphasizing in vivo methods for obtaining the enthalpy—and thereby the energy-storage efficiency—of oxygenic photosynthesis on the millisecond time scale.

6.2.2 Information from Enthalpy and Entropy

As stated in Sect. 6.1, the ΔH and $T\Delta S$ terms in Eq. (6.1) define the basic driving force of the reaction. If ΔH is larger, the driving force is bonding. If $T\Delta S$ is larger, it is the number of states, or the occupation of low-frequency modes, i.e., structural changes from weak intermolecular interactions. For simple chemical reactions, ΔH usually predominates. However, for reactions in the complex solvent, water, or those involving proteins, with their many conformational and ionization states, $T\Delta S$ can compete with or even exceed enthalpic contributions to ΔG. Comparison of ΔG and ΔH therefore immediately distinguishes simple and complex reactions. If $\Delta G \approx \Delta H$ then $T\Delta S \approx 0$, and there is little structural change in the system. If $\Delta G \neq \Delta H$, then the reaction may be complex, possibly involving significant structural change.

Reactions with small ΔG are often considered to be trivial: nothing much happens, one is near equilibrium. However, if in this case one finds a large ΔH (of either sign) then there must be a corresponding large $T\Delta S$ of the same sign. Thus the small observed ΔG may hide large bonding and structural changes that would be missed without this additional information. An example of this is the A_1^--to-$F_{A/B}$ reaction in PSI [29].

In the next section, we discuss PPA and its application to obtain key information on in vivo photosynthesis from direct knowledge of the thermodynamics of photochemistry.

6.3 Pulsed Photoacoustics (PPA) and Photosynthesis

Pulsed PA methods and photosynthesis seem almost to be tailor-made for each other. The typical photosynthetic unit has a very large antenna, consisting of hundreds of photon-collecting molecules that funnel energy to the much smaller reaction center, where photochemistry takes place. Thus the system is easily saturated—i.e., maximally excited with minimal continuous light—and its absorption does not change upon excitation. These intrinsic properties allow the sample used in a PPA measurement to be its own reference [7, 22]. Specifically, PPA requires measuring the total amount of incident pulse energy absorbed by the sample. This can always be done by replacing the sample with a reference that has the same pulsed light absorption, but degrades all the absorbed energy to heat within the resolving time of the apparatus. Photosynthetic samples with the abovementioned properties do just this by themselves when saturated by continuous light in combination with the actinic flashes. A reference is thereby provided without the need for even touching the sample—clearly ideal from an experimental point of view. Isolated reaction centers, or systems with less than a dozen or so antenna molecules, require a separate reference.

We now present an overview of PPA methodology (Sect. 6.3.1) and discuss what can be learned from its application, emphasizing information provided by the energy-storage (E-S) efficiency, ε_{ES}. We then describe a study in which PPA was used to obtain the trap energies and efficiencies of both a common Chl *a* cyanobacterium and the unique Chl *d* species, *A. marina* (Sect. 6.3.2).

6.3.1 PPA Methodology

In PPA, a short (ns–μs) pulse of light shaped as a sheet is directed onto a simple cuvette [30] or a uniform beam into a front-face cell [31] containing a photoactive sample. Following illumination, heat dissipated by the sample generates in the suspending medium a plane sound wave that is detected by a piezoelectric film in a hydrophone (liquid medium) or by a microphone in the air surrounding the sample (air medium). The time scale of measurement is determined by the thickness of the sample, the medium-dependent speed of sound, and the dimensions of the PA cell. Liquid-phase PPA probes 10 ns to 10 μs processes, and air-coupled PPA 100 μs to 100 ms processes.

6.3.1.1 Light Pulses

The required duration of the light pulse depends on the chosen time resolution of the measurement. To measure the complete electron-transfer path of photosynthesis, a few millisecond pulse from a flash lamp is adequate. However, much

more information is available if a spectrally well-defined, shorter duration pulse is used. A Nd:YAG-pumped OPO system is ideal, as the pulse time is a few nanoseconds, and wavelength resolution can be <1 nm (i.e., <0.002 eV). Difficulties with this system include its instability and delicacy of alignment; one can easily spend more time tuning the YAG and aligning the OPO than running the experiment. This problem is now being solved by the availability of pulsed diode lasers with resolution near 1 nm. Obtaining a few μJ pulse in ~10 μs with these lasers requires an output of ≥1 W. Their ease of operation is far superior to that of the YAG-OPO system. However, pulsed diode lasers are currently monochromatic, and thus a new "head" is needed for each experimental wavelength. As the cost of these lasers decreases, multiple-wavelength units will likely become increasingly available.

6.3.1.2 Fast Hydrophone: Liquid-Phase PPA

In fast time-scale PPA, a liquid sample is placed in a front-face PA cell [31] in which the detector is a hydrophone, consisting of a piezoelectric film following a highly reflective mirror at the rear of the cell (Fig. 6.1a). This construction doubles the light path length and isolates the piezo film from the light pulse. The delay of a few μs determined by the speed of sound within the thick mirror usefully isolates electrical artifacts from the pulsed laser or flash lamp. Use of a front-face cell or a light sheet in a simple cuvette ensures a plane acoustic wave and linearity of measurements, which allows deconvolution of the signal and isolation of time-dependent components. The liquid-phase apparatus is highly sensitive and thermostated to accommodate controlled changes in temperature, allowing separation of enthalpic and inherent contributions to observed volume changes [17] (see next section).

Photochemistry-Induced Volume Changes

In PPA, the pressure wave following the light pulse is produced by the volume change (ΔV) of the system, and is therefore proportional to dV/dt. In fast PPA, ΔV has two sources. One is the thermal expansion caused by the heat flux, or ΔH of photochemistry. The other is the volume change inherent to the reactions themselves—notably, in photosynthetic primary reactions, the shrinkage caused by electrostriction on charge separation [17, 32]. By taking advantage of the unique physical properties of water, liquid-phase PPA allows separation of the two components of ΔV. At the temperature of its maximum density (≈4 °C), the thermal expansivity (α) of water is zero, so only inherent volume changes are observed. Assuming that inherent contributions to the total ΔV are constant over a small (≈20 °C) temperature range, additional measurements within this range allow the thermal contributions to be easily obtained from the observed total. To optimize signal-to-noise, one averages many signals following weak flashes and plots the

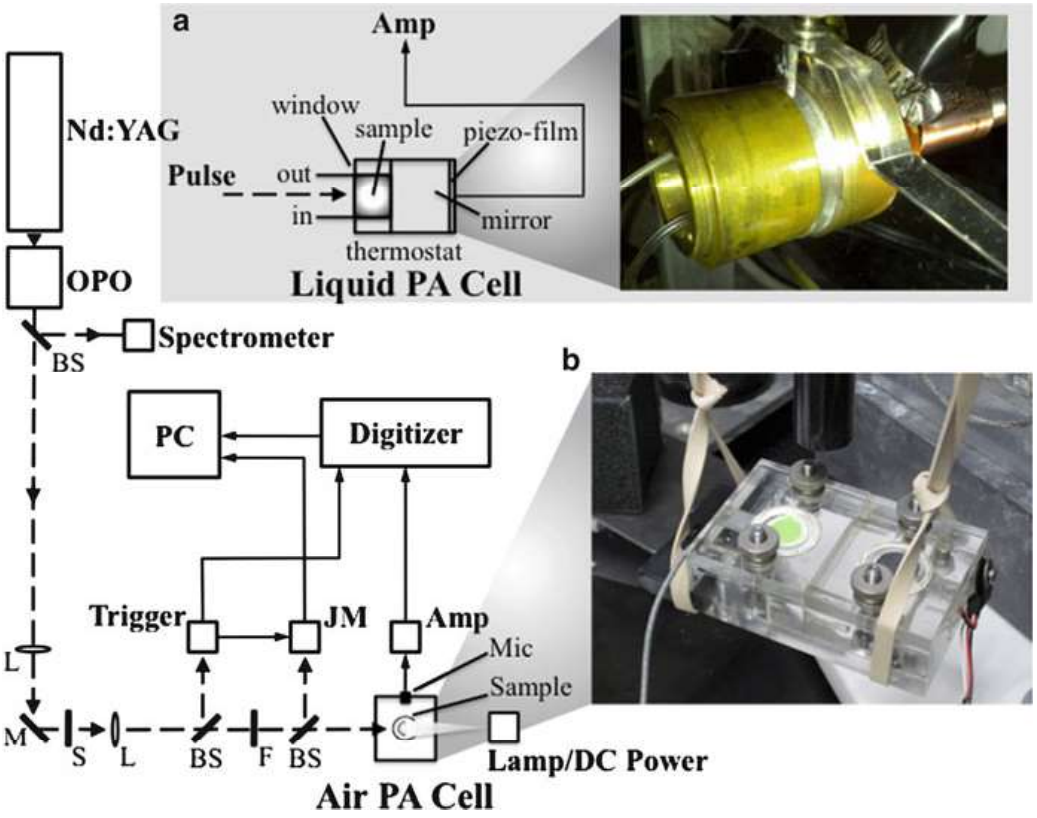

Fig. 6.1 *Fast and slow PPA experimental setups.* (**a**) Setup for ns–μs (solution) PPA. *Nd:YAG* pulsed laser source, *OPO* optical parametric oscillator, *BS* beam splitter, *L* lens, *PD-Trig* (pulsed) diode trigger. Elements of the thermostated hydrophone cell described in the text (Sect. 6.3.1.2) are indicated. (**b**) Setup for millisecond (air) PPA. *M* mirror, *S* shutter, *F* filters, *JM* joulemeter, *Lamp/DC Power* continuous (saturating) light source. Elements of the microphone cell described in the text (Sect. 6.3.1.3) are indicated. The photograph shows the PA cell used in the experiments described in Sect. 6.3.2.1. The cell is suspended by a viscoelastic medium (rubber bands in the setup shown), which absorb external vibrations at least as effectively as costly isolation tables. The black end piece of the optical guide from the saturating lamp is visible at top center. A sample consisting of *A. marina* whole cells on Millipore filter paper is also visible (*green circle*). Measurements of whole cells using this setup provide the enthalpy of in vivo reactions yielding millisecond time-scale products

data—corrected for any changes in compressibility—versus the thermal expansivity of the particular medium used. By normalizing to the reference, the slope of the resulting line is $\Delta H/E_{h\nu}$, and the intercept is $\Delta V/\alpha \times E_{h\nu}$. Details and possible sources of error are discussed in [7, 33].

Knowledge of inherent volume changes can provide important information on the underlying photochemistry. For example, our analysis of electrostriction in bacterial reaction centers using the Drude equation allows an estimation of the dielectric constant of the surrounding protein [34]. Other sources of inherent volume change include conformational changes that create or destroy internal space in the protein. An example of this is seen in the photocycle of bacteriorhodopsin, where such changes make a positive (expansive) contribution to ΔV [35].

Fast PPA In Vivo

Since so much is now known of the kinetics of PSI and PSII, one can use whole cells and PA to determine not only the energetics of "total" photosynthesis but also that of its individual steps. The enormous advantage is that the information is of the interacting photosystems in their natural context, without disruption or addition of deleterious reagents.

The use of intact cells with liquid-phase PPA requires a correction for their internal medium [5]. Depending on the size of the cell, the prompt thermal expansion differs from that of the surrounding water, so two further measurements are required. The time resolution depends on the thickness of the wave-forming volume; it is about 1 μs for a 1 mm thickness. However, data deconvolution procedures allow measurement at 10 % of this resolution [25], and have enabled us to resolve, for instance, the 10 ns formation of the triplet state from B_{860} cation–Bacteriopheophytin anion in quinone-less bacterial reaction centers in a 0.1 mm cell [Edens and Mauzerall, unpublished]. We have determined that the same signal is obtained from light-saturated photosynthetic cells as from a reference material [7]; thus, samples used for fast PPA measurements in vivo can be used as their own reference, as described above.

The long time-range for in vivo liquid-state experiments is limited to about 10 μs, because of the aforementioned proportionality between the acoustic signal and dV/dt; for a given ΔV, a microvolt signal in 1 μs becomes a nanovolt signal in 1 ms. In addition, reflections from any air boundaries in a reasonably sized apparatus lead to a confused signal within a few tens of μs.

6.3.1.3 Slow Microphone: Air PPA

Air PPA employs a simple plexiglass cell where samples are placed in an airtight receptacle, and photoacoustic waves are channeled to a microphone embedded in the cell wall [36] (see Fig. 6.1). The loss of sensitivity on the slower time scale is compensated by the much larger thermal expansivity of air. But this adds the complication of thermal diffusivity in the sample, and thus a depth-dependent signal. Therefore, use of thin samples—such as a leaf, or cells deposited on a thin substrate—is ideal. One can then measure photochemistry of the entire sample in the 10–100 ms time available to commercial microphones. The time resolution can be as high as ≈50 μs [36]. Only heat changes are measured since the large thermal expansivity of air overwhelms the small inherent volume changes. An advantage of ms-time scale PA is that it provides information on complete photosynthesis, at least from oxygen to further than ferrodoxin. Since the detectors are essentially noisy capacitors, a high-impedance FET input amplifier is best. Some air microphones have a built-in FET, allowing the output to be used directly. With low-energy light pulses, essential for obtaining the maximum efficiency of photosynthetic systems (Sect. 6.3.2), averaging of the signal is required. The pulse rate must be checked to ensure that it is not too large a

fraction of the turnover time of the system; however, for very-low-energy light pulses this is less of a problem, because the time required for saturation increases as the fraction of excitation decreases.

This method can be used for in vivo measurements in the 10 ms range. It is principally sensitive to surface effects and thus is ideal for leaves, either real or synthetic. Synthetic leaves consisting of whole-cell cultures affixed to Millipore filter paper have been used to obtain energy-storage efficiencies for the alga *Chlorella vulgaris* [37], and the cyanobacteria *Synechococcus* sp. PCC 7002 [8] and *A. marina* [9, 38] (Sect. 6.3.2.1).

We have developed a robust PA cell that measures the pressure change directly and is useful in the 50 μs-to-1 s time range [39, 40]. This cell has been used to obtain the enthalpy and volume changes of intermediates in the photocycle of bacteriorhodopsin [35]. Arata and Parson [17] used a capacitor cell to make similar measurements, but their results could not be repeated, most likely because the cell was highly sensitive to vibration and electrical interference.

6.3.2 *An Example of the Application of PPA: Determination of the Maximal Energy Yield and Trap Energies of Photosynthesis*

The determination of the quantum yield or the quantum requirement of photochemistry was a major hurdle on the path to understanding photosynthesis [41]. The formidable problem was, and still is, the determination of the absolute light absorption by the heavily light-scattering sample. Photoacoustics bypasses this problem by directly determining the light absorbed, and *only* the light absorbed, by the system. The effect of light scattering is only to reduce and homogenize the incident light intensity. As long as it is the same for the dark measurement (sample is in the dark) and the reference light measurement (sample is saturated by continuous light), the scattered light is irrelevant.

Photoacoustics determines the energy efficiency, not the quantum efficiency. If the enthalpies of the products of the photosynthetic system are known, a given efficiency is easily converted to the other. However, there are two significant advantages to the photoacoustic method. First, one determines *all* the energy stored in the system up to the time of measurement. Thus, in addition to the energy stored in products of photochemistry, that stored in proton gradients and protein conformational changes is measured. In principle, even the formation of ATP can be measured by PA; detection of the pressure wave would be difficult in this case because of the slowness of the reaction, but is likely achievable with the aforementioned pressure cell, which measures into the many-second time range [39, 40]. By contrast, quantum yield experiments measure energy stored in a specific product, such as oxygen or “fixed” carbon dioxide, and so do not capture complete photosynthesis.

A second advantage of PPA over quantum yield experiments is that it has already achieved an accuracy of 99 % [9, 38]. The accuracy of quantum yield measurements is typically no higher than 95 % [42–44]. As discussed in Sect. 6.3.2.1, the combination of accuracy and ability to employ many well-defined excitation wavelengths has allowed PPA measurements of energy-storage efficiencies in vivo that provide unprecedented additional information, including the trap energies and specific efficiencies of PSI and PSII directly from energy measurements [9].

The E-S efficiency at chosen pulse energy and wavelength, ε_{ES}, is defined as that fraction of the absorbed energy that is stored by the sample on the time scale of the PPA measurement:

$$\varepsilon_{ES} \equiv E_{sto}/E_{abs}, \tag{6.2}$$

where E_{sto} and E_{abs} are the energy stored and absorbed. Following a pulse in the dark, the unstored portion of E_{abs} is dissipated as heat (E_{dis}), generating the acoustic wave detected by the microphone within the PA cell. Eq. (6.2) can then be written as

$$\varepsilon_{ES} = (E_{abs} - E_{dis})/E_{abs} = 1 - E_{dis}/E_{abs}. \tag{6.3}$$

When the same sample is continuously illuminated during the experiment, $E_{sto} = 0$ because photochemistry is saturated. Following a pulse in this case, all the absorbed energy is dissipated by the sample ($E_{dis} = E_{abs}$). Thus, as noted above, the reference energy E_{abs} needed to calculate ε_{ES} can be obtained simply by illuminating the sample and repeating the measurement. Moreover, because the pressure waves are proportional to E_{dis}, the PA signals themselves can be directly used to calculate the efficiency:

$$\varepsilon_{ES} = 1 - E_{dis,Dk}/E_{dis,Lt} = 1 - S_{Dk}/S_{Lt}, \tag{6.4}$$

where $E_{dis,Dk}$ and $E_{dis,Lt} = E_{abs}$ are the energies dissipated from the dark (Dk) and illuminated (Lt) sample following a laser pulse, and S_{Dk} and S_{Lt} are the amplitudes (or integrals) of the corresponding signals from the detector (Fig. 6.2).

The observed ε_{ES} at chosen wavelength decreases with increasing flash energy, E, because the flashes themselves saturate the sample. At low (~10 μJ) energies, this decrease is linear [8, 38], allowing the maximal or the ideal (zero-energy) E-S efficiency, $\varepsilon_{ES,max}$, to be obtained from a linear fit to low-E measurements of $\varepsilon_{ES}(E)$ (Fig. 6.2b); that is, $\varepsilon_{ES,max} \equiv \lim_{E_{abs} \to 0} \varepsilon_{ES}$.

The wavelength dependence of ε_{ES} is determined by the trapping energies of the photosystems, $E_t = hc/\lambda_t$, where the trap wavelength λ_t is the photon wavelength corresponding to E_t. When $\lambda < \lambda_t$, absorbed photons are degraded to E_t in subpicoseconds, with the excess energy being dissipated as heat. Then, with the trap at E_t, photochemistry ensues, with a fraction ε_t of E_t being stored and the remainder, corresponding to ΔH, being dissipated. Because the overall efficiency is the stored fraction of the total absorbed energy, the ε_{ES} measured by PPA is

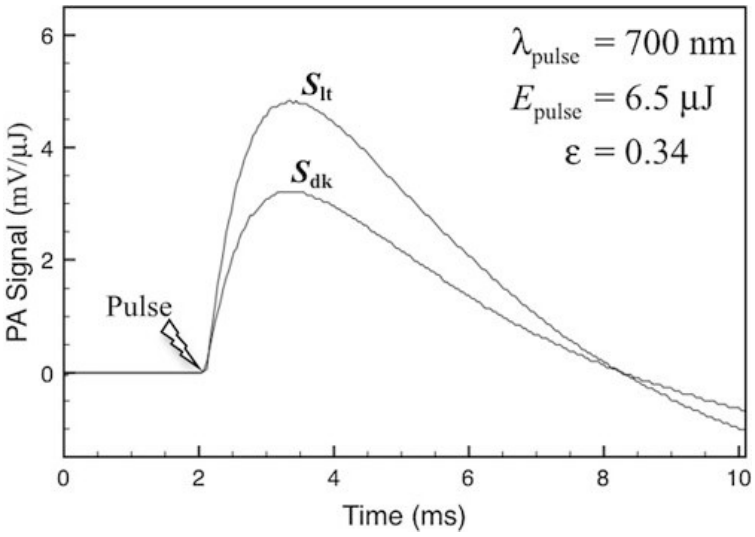

Fig. 6.2 Representative ms-timescale PPA signals, which are the time derivative of the pressure, dP/dt, following illumination of the sample with a laser pulse (Sect. 6.3.1, 6.3.2). S_{dk} and S_{lt} are the amplitudes of averaged signals from an active, dark-adapted *A. marina* sample (0.8 cm^2), and the same sample under continuous saturating light, respectively. The pulse energy (E) is 6.5 μJ and the pulse wavelength (λ_{pulse}) 700 nm. The pulse flashes the sample at 2.05 ms, and the peak of the resulting pressure wave, S_{dk} or S_{lt}, is detected by the microphone at 3.4 ms. The energy-storage efficiency at this flash energy and wavelength, calculated from the amplitudes (Eq. 6.4), is $\varepsilon = 34\,\%$

expected to increase linearly as λ increases to λ_t, and contributions to the observed E_{dis} from light harvesting decrease to zero. For oxygenic photosynthesis, the observed ε_{ES} is usefully complicated by the simultaneous contributions to storage by two photosystems with differing E_t [9] (see below); however, for a given system, one can write

$$\varepsilon_{ES}(\lambda) = (\lambda/\lambda_t)\varepsilon_t. \tag{6.5}$$

Thus, when the pulse wavelength equals the trap wavelength ($\lambda = \lambda_t$), one obtains the E-S efficiency intrinsic to the trap and specific to photochemistry, i.e., the trap efficiency, $\varepsilon_t = \varepsilon_{ES}(\lambda_t)$. For simplicity we are neglecting small losses by fluorescence. The complete equations are given in [37].

When $\lambda > \lambda_t$ ($E < E_t$), excitation of the trap requires uphill energy transfer driven by the thermal bath. In this case, the efficiency actually increases. However, thermodynamics requires an increase of the activation energy of the uphill reaction for increasing $\lambda > \lambda_t$, leading to an exponential slowing. Correspondingly, one expects a drop in energy storage, and therefore in the observed efficiency.

PPA applied at well-resolved wavelengths over a sufficient range provides the detailed spectral behavior of ε_{ES}. It is therefore the ideal—if not the only—methodology for directly identifying the crucial photosystem trap energies of which this behavior is a consequence.

6.3.2.1 Spectral Dependence of the In Vivo Energy-Storage Efficiency in the Chl *d* Cyanobacterium, *Acaryochloris marina*

We recently reported results of PPA measurements of the ms-time scale E-S efficiency in cyanobacterial intact cells over a 90 nm range of pulse wavelengths [9]. As noted, the unprecedented accuracy (1 % error) and wavelength resolution (1 nm or 0.002 eV) of these measurements, combined with the differing efficiencies of PSI and PSII, allow unique fits of a simple model to the data, and thereby provide the trap efficiencies and spectrally dependent fractional absorption of the photosystems. Results include the first direct observation of the PSI and PSII trap energies, which to date have been inferred from other information, typically absorption difference spectra [45]. We next briefly review this effort in order to illustrate both the application of PPA and the information it is able to provide.

The main objective of the study reported in [9] was to obtain the in vivo, wavelength-dependent E-S efficiency (specifically, the maximal wavelength-dependent efficiency, $\varepsilon_{ES,max}(\lambda)$) in the cyanobacterium *Acaryochloris marina*. This species is the only photosynthetic organism known to utilize chlorophyll (Chl) *d* as its primary photopigment [46]. In Chl *d*, a vinyl-to-formyl substitution redshifts the Q_Y absorption peak of Chl *a* by ≈40 nm (i.e., to ≈710 nm) in vivo, enabling *A. marina* to perform oxygenic phototrophy in niche environments enhanced in far-red/near-IR light [46–48]. *A. marina*'s viability in these low-photon-energy environments, and the presence of Chl *d* in its reaction centers [49], indicate that Chl *a*—otherwise ubiquitous among oxygenic species—is not a categorical requirement of water-utilizing photosynthesis. Determining $\varepsilon_{ES,max}(\lambda)$ in *A. marina* and comparing with that in Chl *a* species address the extent to which photochemistry in the former is thermodynamically limited by its use of Chl *d*, and potentially elucidate fundamental constraints on electron transfer in oxygenic photosynthesis. This question of the "long-wavelength limit" for O_2 formation by water-utilizing photochemistry [3, 9, 38, 50] is of considerable interest to a broad range of research areas, including basic photosynthesis, evolutionary biology, renewable energy, and astrobiology.

PPA employing an air microphone (Sect. 6.3.1.3) was used to obtain reaction enthalpies from *A. marina* whole-cell samples on a time scale of ≈3 ms (see Fig. 6.2). By referencing to the enthalpies measured when the same samples were saturated by continuous light, we obtained the in vivo E-S efficiency of photochemistry from formation of oxygen to beyond formation of ferrodoxin [51]. The λ dependence of the efficiency is directly determined by the wavelengths (exciting photon energies) of the photosystem traps, $\lambda_{t,I}$ (PSI) and $\lambda_{t,II}$ (PSII). If (and only if) these have different efficiencies, they can be directly identified from accurate measurements of $\varepsilon_{ES,max}$ at well-resolved wavelengths in the spectral region encompassing $\lambda_{t;I,II}$. For *A. marina*, we determined $\varepsilon_{ES,max}$ at 5 nm intervals from $\lambda = 670$ to 760 nm. By then fitting to the data a model that contains the dependence of $\varepsilon_{ES,max}(\lambda)$ on the absorption of each photosystem, and also on

the absorbed pulse wavelength relative to the trap wavelengths (Sect. 6.3.2), we obtained the trap energy, E_t, and efficiency, ε_t, for both photosystems. By incorporating an exponential factor to accommodate uphill energy transfer, the model also captures observed decays in the efficiency following both $\lambda_{t,II}$ and $\lambda_{t,I}$. For comparison, we additionally determined $\varepsilon_{ES,max}(\lambda)$ at 5 nm intervals from $\lambda = 670$ to 725 nm in whole cells of the Chl *a* cyanobacterium, *Synechococcus leopoliensis*.

The principal conclusions of [9] include the following: (1) The efficiency in *A. marina* (*Am*) exceeds that in *S. leopoliensis* (*Sl*) by ≈5 % at the respective peak absorption wavelengths, consistent with the higher efficiency expected if *Am* forms the same products as *Sl* from a lower energy initial state. (2) The efficiency in *Am* at the trap wavelengths (32 % at 723 nm [PSII], 43 % at 740 nm [PSI]) also exceeds that in *Sl* (30 % at 671 nm [PSII], 38 % at 695 nm [PSI]). These values confirm previously reported high efficiencies of primary reactions in both photosystems, with that of PSI exceeding that of PSII [37, 38]. The fitted values of both trap wavelengths in *Am* are >40 nm longer than those in *Sl*; the values in both species agree with previous spectroscopy-derived values within the error [45, 52, 53]. (3) The result $\lambda_{t,II} = 723$ nm in *Am* supports evidence that the primary electron donor is a Chl *d* monomer at the active-branch accessory site (Chl_{D1}) [53–55]. Additionally, one finds that the contribution of phycobilins to overall energy storage by PSI in *Am* is <10 % of the contribution to PSII. By contrast, the corresponding data indicate that in *Sl* these pigments contribute approximately equally to storage in both photosystems, consistent with previous results [56].

Figure 6.3 shows the spectral efficiencies ($\varepsilon_{max}(\lambda)$) of *A. marina* and *S. leopoliensis* reported in [9] (filled circles and open squares, respectively). The *Am* dataset includes revised efficiencies between 722.5 and 735 nm (gray filled circles), and a revised fit (thick solid curve). Figure 6.3 also shows absorbance (Abs) spectra of *Am* and *Sl* whole-cell samples used in the efficiency measurements (filled circles and open squares). The revised fit to the *Am* efficiencies incorporates a revised fit of the underlying PSI and PSII absorption bands to the observed absorbance spectrum (open triangles). The revised efficiency fit yields the same values of $\lambda_{t,II}$ and $\varepsilon_{t,II}$ obtained from the fit reported in [9] (dashed curved in Fig. 6.3)—i.e., $\lambda_{t,II}$ = 723 nm, $\varepsilon_{t,II}$ = 0.32—and the slightly revised values $\lambda_{t,I}$ = 737 nm, and $\varepsilon_{t,I}$ = 0.46, with comparable uncertainties (<∼ 5 %) and a slightly smaller overall root-mean-square error— 1.0 % vs. 1.3 %. For a detailed description of the efficiency model and fitting procedure, see the appendix in [9].

In addition to illustrating the utility of PPA, these results establish that energy storage via water-utilizing photosynthesis in *A. marina* is not thermodynamically limited by its use of far-red (to ≈750 nm) photons to initiate the primary reactions, indicating that oxygenic phototrophy is likely viable in even redder light environments. The significance of this is far reaching. For example, in the context of renewable energy research, it means that *A. marina* has adapted photochemistry in a way that has allowed it to significantly increase the solar-energy conversion efficiency [3] (Sect. 6.1) and simultaneously preserve the energy-storage efficiency [38]. Further study will therefore potentially inform efforts leading to optimally efficient, water-utilizing solar fuel technologies.

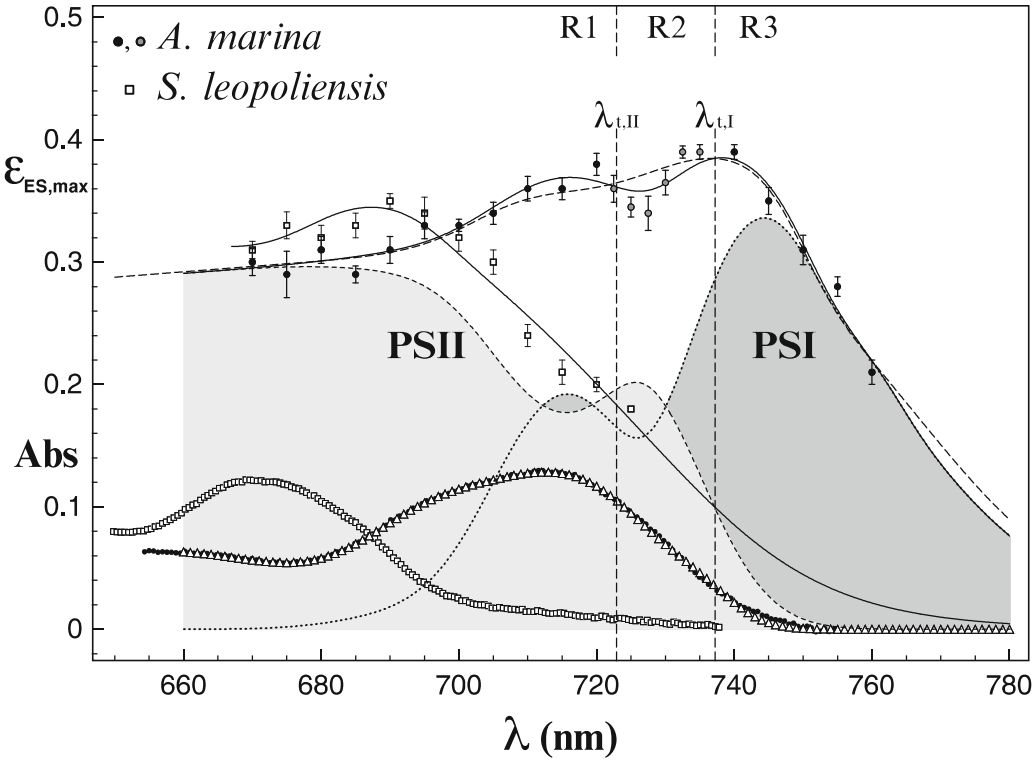

Fig. 6.3 Spectral dependence of the maximum energy-storage efficiency, $\varepsilon_{ES,max}(\lambda)$, in *A. marina* (black and gray filled circles) and *S. leopoliensis* (open squares) (see Sect. 6.3.2.1). Gray circles update the *Am* data reported in [9]. The error bar at each experimental wavelength, λ, is the rms deviation of a linear fit of ε_{ES} measurements versus pulse energy E to obtain $\varepsilon_{ES,max}$ (Sect. 6.3.2; the result shown in Fig. 2 corresponds to one point in the ε_{ES} vs. E dataset at $\lambda = 700$ nm). Thick and thin solid curves are fits to the ε_{max} data using the model described in Sect. 6.3.2.1 and [9], which assumes the PSI and PSII traps, $\lambda_{t;I,II}$, define three spectral regimes of the observed efficiency, R1, R2, and R3 (indicated for *A. marina* at top of figure), providing the photosystem-specific trap energies and efficiencies of the two cyanobacteria. The revised *A. marina* fit (RMS error = 1.0 %, 95 % confidence interval) improves on the best previously obtained fit (dashed curve; RMSE = 1.3 %) [9]. Also shown (reproduced from Ref. [9]) are absorbance (Abs) spectra of *A. marina* and *S. leopoliensis* intact-cell PPA samples; the *A. marina* absorbance fit (open triangles) corresponding to the revised efficiency fit; and the specific, λ-dependent contributions of PSI and PSII to the modeled total efficiency (labeled dashed and dotted curves with bounded areas shaded for clarity)

6.4 Conclusions

Pulsed photoacoustics is the ideal experimental method for probing the thermodynamics of photosynthesis over an extended time scale. It is one of only a few related methods able to directly measure energy changes in electron-transport processes, and is arguably the most elegant, accurately resolving photochemical enthalpy and volume changes simply by detecting the resulting acoustic wave using a microphone.

Likewise, photosynthetic systems are an ideal subject for PPA. Their large and efficient antennae allow for easy saturation of the sample with negligible change in absorption, providing an internal reference and thereby a high degree of accuracy. Samples can consist either of whole cells, providing information on in vivo photosynthesis, or of isolated thylakoid membranes or photosystem complexes, providing more specific information.

Because the temporal resolution of PPA is determined by the speed of sound in the sample medium and the dimensions of the PA cell, reactions on time scales spanning many orders of magnitude—from early photochemistry (nanoseconds) to almost complete photosynthesis (~100 ms)—can be studied. The list of information available is long; examples we have emphasized here include the following:

1. Details of thermodynamics to complement the much more extensive existing knowledge of kinetics and structure: In particular, the enthalpy and volume changes both of overall photosynthesis and of individual reaction steps in the electron-transport chain can be determined. In the latter case, time constants can be used to assign the measured changes to a specific, spectrally identified reaction. Where the free energy is known, one can also obtain entropy changes, which are of great interest because they provide insight into important but often overlooked structural contributions to energy storage.
2. With knowledge of the enthalpy, and taking advantage of the self-calibration possible with photosynthetic samples, the thermal (energy-storage) efficiency at chosen pulse energy and wavelength can be determined to an accuracy of 1 %. Linear fitting to efficiency measurements over a range of low-pulse energies provides the maximal energy-storage efficiency of the system. Experiments employing intact cells provide the overall efficiency in vivo. In oxygenic systems, the differing intrinsic efficiencies of the PSI and PSII traps allow in vivo measurements over a range of well-resolved pulse wavelengths to provide the specific contributions of the photosystems to the observed efficiency. This eliminates the need for difficult isolation and purification procedures; captures the separate efficiencies of the photosystems in their natural, interactive context; and further illustrates the incredible suitability of photosynthetic systems for investigation by PPA.
3. Importantly, obtaining the in vivo efficiency as a function of pulse wavelength also provides the unique trap energies of the photosystems *directly from energy measurements*. These are in contrast to conventional approximations of the trap energy obtained from absorption difference spectroscopy. The spectral dependence of the efficiency additionally provides information on energy-transfer processes for absorbed photon energies higher or lower than those of the traps, such as the thermodynamically limited uphill transfer of lower energy excitations.
4. Extensive additional information available to PPA includes system turnover times, quantum yields, optical cross sections, and, in the case of oxygenic photosynthesis in leaves, rates and yields of O_2 formation.

Thus, pulsed photoacoustics is a unique, simple, and powerful tool for investigating the thermodynamics of electron transport in photosynthetic systems.

Acknowledgements We gratefully acknowledge our collaborators, Dr. N. Y. Kiang and Prof. R. E. Blankenship, for their invaluable contributions to the work described in Sect. 6.3.2.1, as well as the technical expertise of Irena Zielinski-Large. We also acknowledge the NASA Astrobiology Institute (NAI), Prof. V. S. Meadows (Univ. of Washington, PI of the Virtual Planetary Laboratory Lead Team, NAI), and Dr. Carl Pilcher (Former Director, NAI) for support under Cooperative Agreement No. NNA08CN87A and the Director's Discretionary Fund program. SPM additionally acknowledges the NASA Postdoctoral Program (NPP) and NAI for support by an NAI NPP fellowship.

References

1. Dau H, Zaharieva I. Principles, efficiency, and blueprint character of solar-energy conversion in photosynthetic water oxidation. Acc Chem Res. 2009;42:1861–70.
2. Blankenship RE, Tiede DM, Barber J, Brudvig GW, Fleming G, Ghirardi M, Gunner MR, Junge W, Kramer DM, Melis A, Moore TA, Moser CC, Nocera DG, Nozik AJ, Ort DR, Parson WW, Prince RC, Sayre RT. Comparing photosynthetic and photovoltaic efficiencies and recognizing the potential for improvement. Science. 2011;332:805–9.
3. Chen M, Blankenship RE. Expanding the solar spectrum used by photosynthesis. Trends Plant Sci. 2011;16:427–31.
4. Barber J. Photosynthetic energy conversion: natural and artificial. Chem Soc Rev. 2009;38:185–96.
5. Boichenko VA, Hou JM, Mauzerall D. Thermodynamics of electron transfer in oxygenic photosynthetic reaction centers: volume change, enthalpy, and entropy of electron-transfer reactions in the intact cells of the cyanobacterium Synechocystis PCC 6803. Biochemistry. 2001;40:7126–32.
6. Hou JM, Boichenko VA, Diner BA, Mauzerall D. Thermodynamics of electron transfer in oxygenic photosynthetic reaction centers: volume change, enthalpy, and entropy of electron-transfer reactions in manganese-depleted photosystem II core complexes. Biochemistry. 2001;40:7117–25.
7. Hou JM, Boichenko VA, Wang YC, Chitnis PR, Mauzerall D. Thermodynamics of electron transfer in oxygenic photosynthetic reaction centers: a pulsed photoacoustic study of electron transfer in photosystem I reveals a similarity to bacterial reaction centers in both volume change and entropy. Biochemistry. 2001;40:7109–16.
8. Charlebois D, Mauzerall D. Energy storage and optical cross-section of PS I in the cyanobacterium Synechococcus PCC 7002 and a psaE− mutant. Photosynth Res. 1999;59:27–38.
9. Mielke SP, Kiang NY, Blankenship RE, Mauzerall D. Photosystem trap energies and spectrally-dependent energy-storage efficiencies in the Chl *d*-utilizing cyanobacterium, *Acaryochloris marina*, Biochim Biophys Acta. 2013;1827:255–265.
10. Mauzerall D. Thermodynamics of photosystem I. In: Golbeck JH, editor. Photosystem I: the light-driven plastocyanin: ferredoxin oxidoreductase. Dordrecht, The Netherlands: Springer; 2006. p. 571–81.
11. Mauzerall D, Feitelson J, Prince RC. Wide-band time-resolved photoacoustic study of electron-transfer reactions: difference between measured enthalpies and redox free energies. J Phys Chem. 1995;99:1090–3.
12. Parson WW. Thermodynamics of the primary reactions of photosynthesis. Photochem Photobiol. 1978;28:389–93.

13. Woodbury NW, Allen JP. The pathway, kinetics and thermodynamics of electron transfer in wild type and mutant reaction centers of purple nonsulfur bacteria. In: Blankenship RE, Madigan MT, Bauer CE, editors. Anoxygenic photosynthetic bacteria. The Netherlands: Kluwer Academic; 1995. p. 527–57.
14. Parson WW. Photosynthetic bacterial reaction centers: interactions among the bacteriochlorophylls and bacteriopheophytins. Annu Rev Biophys Bioeng. 1982;11:57–80.
15. Xu Q, Gunner MR. Temperature dependence of the free energy, enthalpy and entropy of P+QA- charge recombination in Rhodobacter sphaeroides R-26 reaction centers. J Phys Chem. 2000;104:8035–43.
16. de Winter A, Boxer SG. Energetics of primary charge separation in bacterial photosynthetic reaction center mutants: triplet decay in large magnetic fields. J Phys Chem A. 2003;107:3341–50.
17. Arata H, Parson WW. Enthalpy and volume changes accompanying electron transfer from P-870 to quinones in Rhodopseudomonas sphaeroides reaction centers. Biochim Biophys Acta. 1981;636:70–81.
18. Brettel K. Electron transfer and arrangement of the redox cofactors in photosystem I. Biochim Biophys Acta. 1997;1318:1869–77.
19. McMahon BH, Muller JD, Wraight CA, Nienhaus GU. Electron transfer and protein dynamics in the photosynthetic reaction center. Biophys J. 1998;74:2567–87.
20. Havaux M, Lorrain L, Leblanc RM. Photothermal beam deflection: a new method for in vivo measurements of thermal energy dissipation and photochemical energy conversion in intact leaves. Photosynth Res. 1990;24:63–73.
21. Terazima M. Enthalpy change and reaction volume of photochemical reactions measured by the transient grating method. Trends Photochem Photobiol. 1997;4:1–11.
22. Malkin S, Cahen D. Photoacoustic spectroscopy and radiant energy conversion: theory of the effect with special emphasis on photosynthesis. Photochem Photobiol. 1979;29:803–13.
23. Havaux M, Canaani O, Malkin S. Photosynthetic responses of leaves to water stress, expressed by photoacoustics and related methods: I. Probing the photoacoustic method as an indicator for water stress in vivo. Plant Physiol. 1986;82:827–33.
24. Braslavsky SE, Heibel GE. Time-resolved photothermal and photoacoustic methods applied to photoinduced processes in solution. Chem Rev. 1992;92:1381–410.
25. Feitelson J, Mauzerall D. Photoacoustic evaluation of volume and entropy changes in energy and electron transfer. Triplet state porphyrin with oxygen and naphthoquinone-2-sulfonate. J Phys Chem. 1996;100:7698–703.
26. Delosme R. On some aspects of photosynthesis revealed by photoacoustic studies: a critical evaluation. Photosynth Res. 2003;76:289–301.
27. Mesquita RC, Mansanares AM, Silva ECD, Barja PR, Miranda LCM, Vargas H. Open photoacoustic cell: applications in plant photosynthesis studies. Instr Sci Technol. 2006;34:33–58.
28. Hou HJ, Mauzerall D. Listening to PS II: enthalpy, entropy, and volume changes. J Photochem Photobiol Biol B. 2011;104:357–65.
29. Hou HJ, Mauzerall D. The A-Fx to F(A/B) step in synechocystis 6803 photosystem I is entropy driven. J Am Chem Soc. 2006;128:1580–6.
30. Feitelson J, Mauzerall D. Wide-band, time-resolved photoacoustic study of electron-transfer reactions: photoexcited magnesium porphyrin and quinones. J Phys Chem. 1993;97:8410–3.
31. Arnaut LG, Caldwell RA, Elbert JE, Melton LS. Recent advances in photoacoustic calorimetry: theoretical basis and improvements in experimental design. Rev Sci Instrum. 1992;63:5381–9.
32. Feitelson J, Mauzerall D. Enthalpy and electrostriction in the electron-transfer reaction between triplet zinc uroporphyrin and ferricyanide. J Phys Chem B. 2002;106:9674–8.
33. Edens GJ, Gunner MR, Xu Q, Mauzerall D. The enthalpy and entropy of reaction for formation of P+QA- from excited reaction centers of *Rhodobacter sphaeroides*. J Am Chem Soc. 2000;122:1479–85.

34. Mauzerall D, Hou JM, Boichenko VA. Volume changes and electrostriction in the primary photoreactions of various photosynthetic systems: estimation of dielectric coefficient in bacterial reaction centers and of the observed volume changes with the Drude-Nernst equation. Photosynth Res. 2002;74:173–80.
35. Liu Y, Edens GJ, Grzymski J, Mauzerall D. Volume and enthalpy changes of proton transfers in the bacteriorhodopsin photocycle studied by millisecond time-resolved photopressure measurements. Biochemistry. 2008;47:7752–61.
36. Mauzerall DC. Determination of oxygen emission and uptake in leaves by pulsed, time resolved photoacoustics. Plant Physiol. 1990;94:278–83.
37. Cha Y, Mauzerall DC. Energy storage of linear and cyclic electron flows in photosynthesis. Plant Physiol. 1992;100:1869–77.
38. Mielke SP, Kiang NY, Blankenship RE, Gunner MR, Mauzerall D. Efficiency of photosynthesis in a Chl d-utilizing cyanobacterium is comparable to or higher than that in Chl a-utilizing oxygenic species. Biochim Biophys Acta. 2011;1807:1231–6.
39. Edens GJ, Liu Y, Grzymski J, Mauzerall D. Pressure cell for time-resolved calorimetric measurements of photoinitiated reactions on the fractional millisecond and longer time scale. Rev Sci Instrum. 2003;74:2523–9.
40. Mauzerall D, Liu Y, Edens GJ, Grzymski J. Measurement of enthalpy and volume changes in photoinitiated reactions on the ms timescale with a novel pressure cell. Photochem Photobiol Sci. 2003;2:788–90.
41. Nickelsen K, Govindjee. The maximum quantum yield controversy: Otto Warburg and the "Midwest-Gang". Bern: Institut F R Philosophie; 2011.
42. Dutton PL, Leigh JS, Wraight CA. Direct measurement of the midpoint potential of the primary electron acceptor in Rhodopseudomonas spheroides in situ and in the isolated state: some relationships with pH and o-phenanthroline. FEBS Lett. 1973;36:169–73.
43. Popovic ZD, Kovacs GJ, Vincett PS, Alegria G, Dutton PL. Electric-field dependence of the quantum yield in reaction centers of photosynthetic bacteria. Biochim Biophys Acta. 1986;851:38–48.
44. Cho HM, Mancino LJ, Blankenship RE. Light saturation curves and quantum yields in reaction centers from photosynthetic bacteria. Biophys J. 1984;45:455–61.
45. Blankenship RE. Molecular mechanisms of photosynthesis. Oxford: Blackwell; 2002.
46. Miyashita H, Ikemoto H, Kurano N, Adachi K, Chihara M, Miyachi S. Chlorophyll d as a major pigment. Nature. 1996;383:402.
47. Swingley WD, Chen M, Cheung PC, Conrad AL, Dejesa LC, Hao J, Honchak BM, Karbach LE, Kurdoglu A, Lahiri S, Mastrian SD, Miyashita H, Page L, Ramakrishna P, Satoh S, Sattley WM, Shimada Y, Taylor HL, Tomo T, Tsuchiya T, Wang ZT, Raymond J, Mimuro M, Blankenship RE, Touchman JW. Niche adaptation and genome expansion in the chlorophyll d-producing cyanobacterium Acarylochloris marina. Proc Natl Acad Sci U S A. 2008;105:2005–10.
48. Miller SR, Augustine S, Le Olson T, Blankenship RE, Selker J, Wood AM. Discovery of a free-living chlorophyll d-producing cyanobacterium with a hybrid proteobacterial/cyanobacterial small-subunit rRNA gene. Proc Natl Acad Sci U S A. 2005;102:850–5.
49. Tomo T, Allakhverdiev SI, Mimuro M. Constitution and energetics of photosystem I and photosystem II in the chlorophyll d-dominated cyanobacterium Acaryochloris marina. J Photochem Photobiol B. 2011;104:333–40.
50. Pettai H, Oja V, Freiberg A, Laisk A. The long-wavelength limit of plant photosynthesis. FEBS Lett. 2005;579:4017–9.
51. Cassan N, Lagoutte B, Setif P. Ferredoxin-NADP + reductase. Kinetics of electron transfer, transient intermediates, and catalytic activities studied by flash-absorption spectroscopy with isolated photosystem I and ferredoxin. J Biol Chem. 2005;280:25960–72.
52. Hu Q, Miyashita H, Iwasaki I, Kurano N, Miyachi S, Iwaki M, Itoh S. A photosystem I reaction center driven by chlorophyll d in oxygenic photosynthesis. Proc Natl Acad Sci U S A. 1998;95:13319–23.

53. Schlodder E, Cetin M, Eckert HJ, Schmitt FJ, Barber J, Telfer A. Both chlorophylls a and d are essential for the photochemistry in photosystem II of the cyanobacteria, Acaryochloris marina. Biochim Biophys Acta. 2007;1767:589–95.
54. Cser K, Deak Z, Telfer A, Barber J, Vass I. Energetics of photosystem II charge recombination in Acaryochloris marina studied by thermoluminescence and flash-induced chlorophyll fluorescence measurements. Photosynth Res. 2008;98:131–40.
55. Renger T, Schlodder E. The primary electron donor of photosystem II of the cyanobacterium Acaryochloris marina is a chlorophyll d and the water oxidation is driven by a chlorophyll a/chlorophyll d heterodimer. J Phys Chem B. 2008;112:7351–4.
56. Kondo K, Ochiai Y, Katayama M, Ikeuchi M. The membrane-associated CpcG2-phycobilisome in synechocystis: a new photosystem I antenna. Plant Physiol. 2007;144:1200–10.